Journal of Cleaner Production 319 (2021) 128686

Contents lists available at ScienceDirect

Journal of Cleaner Production

journal homepage: www.elsevier.com/locate/jclepro

Design and optimization of electrodialysis process parameters for brackish water treatment

Dipak Ankoliya [a], Anurag Mudgal [a,*], Manish Kumar Sinha [b], Philip Davies [c], Edxon Licon [d], Rubén Rodríguez Alegre [d], Vivek Patel [a], Jatin Patel [a]

[a] Department of Mechanical Engineering, Pandit Deendayal Energy University, Gandhinagar, Gujarat, India
[b] Department of Chemical Engineering, Pandit Deendayal Energy University, Gandhinagar, Gujarat, India
[c] School of Engineering, University of Birmingham, Edgbaston, UK
[d] Circular Economy Business Unit, LEITAT, Terrassa, Barcelona, Spain

ARTICLE INFO

Handling editor: Bin Chen

Keywords:
Electrodialysis
Water desalination
Design and optimization
Flow velocity
Cell-pair thickness

ABSTRACT

Effect of flow velocity and cell-pair thickness in electrodialysis (ED) is studied. The production cost includes pump energy, while the size of the system is considered as an output variable. The performance of ED system depends on three categories of process parameters namely water quality data, stack configuration and flow characteristic inside the stack. The design of ED system is complex due to interrelation among the system variables so the design calculation chronology steps are developed with flow-chart for the fix feed salinity of groundwater and salt removal rate. The effect of recovery ratio on capital and energy cost is studied and found unidirectional. Sparingly soluble salt present in feed decides the upper limit and obtained 70–75% recovery rate based on the feedwater quality. The optimum value of the linear flow velocity and cell-pair thickness can be obtained by the trade-off among capital cost, stack energy cost and pumping energy cost. Simultaneous effect of both the variable on minimizing the total cost gives the narrow working range of flow velocity 15–17 cm/s and 0.4–0.8 mm thickness. The minimum production cost of 0.08 USD/m^3 is obtained at 16 cm/s velocity and 0.5 mm thickness.

1. Introduction

In India, 73% of villages using groundwater as their primary source of drinking water and around 60% of land in India having brackish groundwater (Wright et al., 2015) while this problem is more severe in north-west states of Gujarat and Rajasthan (Fig. 1). Only in the state of Gujarat, around 18% of area is affected with salinity over 3200 μS/cm electrical conductivity (CGWB-WCR Ahmedabad, 2016) and salinity map is shown in Fig. 2. Brackish water desalination can provide the solution to this groundwater salinity problem (Hanrahan et al., 2016). The membrane technology has played an important role in desalination due to their effectiveness, low energy consumption and cost than thermal desalination (Al-Amshawee et al., 2020). The most common membrane technology in brackish water desalination is reverse osmosis (RO), with 60–90% of the market share depending on location (Campione et al., 2018; He et al., 2018b). ED is gaining attention of researchers, although electrodialysis has possessed only 4% of total installed desalination capacity far behind the RO technology which has possessed 64% (Al-Amshawee et al., 2020; AlMarzooqi et al., 2014), because of the high recovery of water, less sensitivity to the change in feedwater quality and lower specific energy consumption (SEC) of the ED process for brackish groundwater desalination compare to the pressure intensive RO process.

Brackish water desalination for inland water has its own limitation to create it as a water resource for example, the amount of concentrate stream with more salinity than feedwater coming from the desalination process would not be a cost effective and environment friendly solution if disposed inland. The higher recovery brackish water desalination system is required to reduce waste management and cost of disposal (Malmrose et al., 2004; Nicot and Chowdhury, 2005; Watson et al., 2003).

Electrodialysis is particularly suited for high recovery rates up to 95% and high brine concentrations can be achieved (Strathmann, 2010).

* Corresponding author.
E-mail addresses: dipak.personal77@gmail.com (D. Ankoliya), anurag.mudgal@sot.pdpu.ac.in (A. Mudgal), manish.sinha@sot.pdpu.ac.in (M.K. Sinha), p.a.davies@bham.ac.uk (P. Davies), elicon@leitat.org (E. Licon), rrodriguez@leitat.org (R.R. Alegre), VivekP@sot.pdpu.ac.in (V. Patel), Jatin.Patel@spt.pdpu.ac.in (J. Patel).

https://doi.org/10.1016/j.jclepro.2021.128686
Received 5 March 2021; Received in revised form 4 August 2021; Accepted 16 August 2021
Available online 19 August 2021

To achieve high water recovery, it is necessary to control the precipitation of sparingly soluble salt like $CaSO_4$. It is investigated that electrodialysis reversal can achieve higher tolerable $CaSO_4$ saturation level compared to the RO process due to system's electrochemical behavior (Hanrahan et al., 2016; Turek and Dydo, 2003).

ED can be an economical process among the existing brackish water desalination process if used within a specific range of feedwater salinity (Strathmann, 2010). Experimental study for the feedwater salinity below 3000 ppm shows that ED has an economic advantage over RO (Walha et al., 2007) and demonstrated that 75% less energy is consumed by ED at 1000 ppm (Ali et al., 2018). Usage of solar photovoltaic (PV) energy also favors the ED process by the fact that ED can use direct electric current as energy input. Comparative study of PV based ED and RO system concluded that ED requires less energy than RO for the feedwater conductivity around 1700 μS/cm (Karimi et al., 2015). It is also possible to reduce further energy consumption by using some innovative membrane stack configurations (Chen et al., 2020). Comparison of electro-driven technologies based on Nernst-Planck theoretical model shows that ED has lower energy consumption than constant-current membrane capacitive deionization (MCDI) for the similar brackish water desalination conditions (Patel et al., 2020).

ED has flexibility to control product water quality more easily compared to other desalination technologies because salt removal capacity of ED stack directly related to applied voltage which is controlled as an operating parameter (Karimi et al., 2018). In terms of robustness, ED can tolerate silica and biological growth compared to RO (Hanrahan et al., 2016). It can also tolerate higher turbidity due to open channel construction of ED stack (Landsman et al., 2020; Murray, 1995; Walker et al., 2014). ED membranes are less prone to bio-fouling by using higher amount of chlorine because ED membrane is more chlorine resistant than RO membrane (He et al., 2018a; Karimi et al., 2015; Landsman et al., 2020). Long term experimental study at pilot scale by Ghyselbrecht at el. (2013) demonstrated that $CaSO_4$ scaling in concentrate stream was successfully eliminated by using monovalent selective ion exchange membrane in ED (Ghyselbrecht et al., 2013).

At both ends of ED membrane stack, metal electrodes are placed to allow direct electric current from the source and complete the electric circuit. Electrodes are generally made up of titanium metal due to corrosive acid produced from anode compartment and coated with chemically inert platinum metal (Murray, 1995). The other coating material like ruthenium was also used by the researcher (Qu and Liu, 1983) with and without iridium and titanium in composition with coating material to test the life expectancy of electrode. Ruthenium coating containing iridium and more titanium shows the more service life and performance for ED process (Myint et al., 2010; Qu and Liu, 1983). Carbon electrode is also built and tested at lab-scale by He et al. (2018a) but not fulfilling the basic requirement, as the electrodes were having brittle and corrosive in nature (He et al., 2018a).

The design of ED system requires many parameters to be decided based on the selection of geometrical parameter and material of ED stack parts like membrane, spacer and electrode. Apart from these fixed parameters, the variable parameters like feed and product water composition, velocity of water in stack, recovery ratio, electrical parameters etc. are also affect the performance and economics of ED system (Tsiakis and Papageorgiou, 2005).

Some of the previous studies was on optimization of parameters to

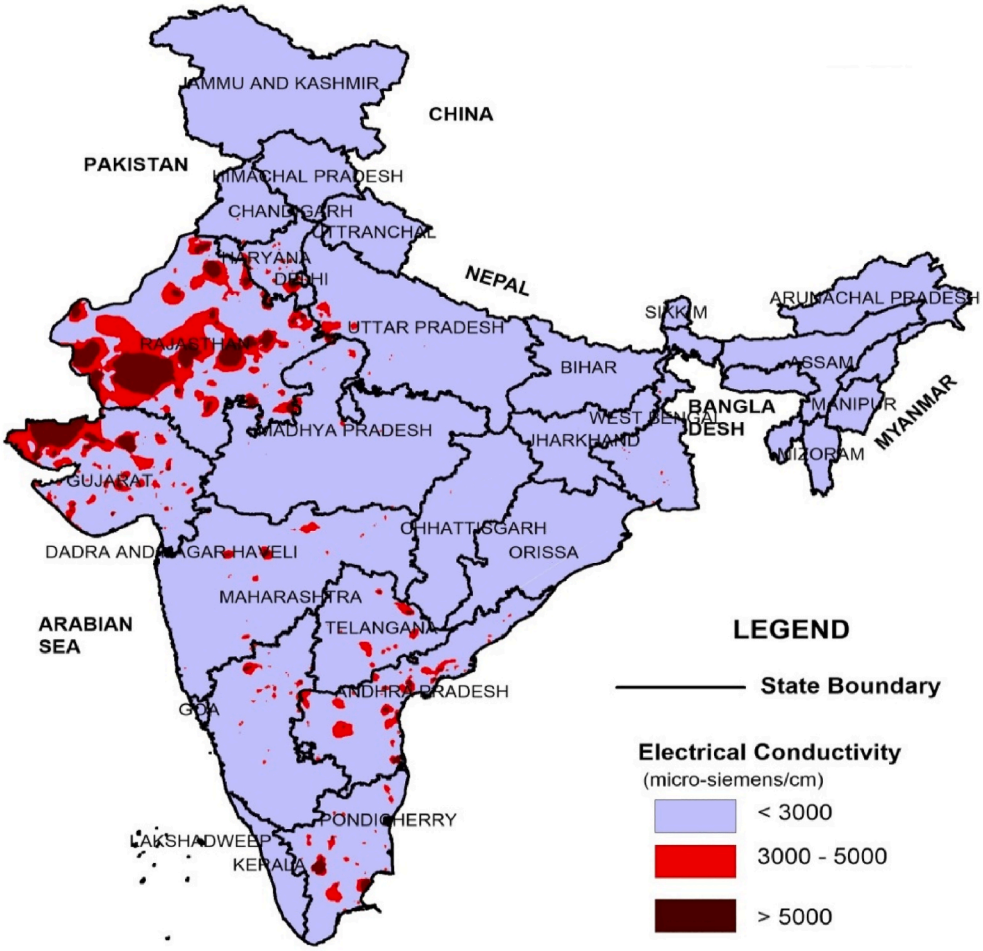

Fig. 1. Map of salinity levels in India (CGWB Faridabad, 2018).

improve the efficiency of the developed and fix sized ED system. The effect of applied voltage, superficial velocity, and temperature of feedwater on ion removal shown by Karimi and Ghassemi (2016) and found that velocity has overall negative effect on ion removal due to decreased ion residence time (Karimi and Ghassemi, 2016). Qureshi et al. (2021) found that flow velocity is most sensitive parameter for current density and specific energy consumption by using the normalized sensitivity analysis for various parameters (Qureshi et al., 2021). In present study, effect of flow velocity as operating parameter is explored on the pressure drop, current density, voltage as energy cost and stack length, membrane area as fixed cost to find minimum possible production cost.

Chehayeb et al. (2017) studied the velocity and channel height on energy consumption for large-scale system for high salinity and brackish water of 3 g/L feed concentration but considers fix sized system (Chehayeb et al., 2017). Shah et al. (2018) has carried out cost optimization with current density for batch mode small scale (9–15 L/h) ED system (Shah et al., 2018). Simplified mathematical model for brackish water ED was developed by Lee at el. (2002) and channel height with current density was optimized by cost but pumping power taken as fix value (Lee et al., 2002).

In this study, the design calculation steps with flow chart is developed including the energy consumption by stack and pump for the fix salt removal rate and feed salinity for the groundwater data of Pandit Deendayal Energy University (PDEU), Gandhinagar, Gujarat, India site as a case study. The effect of recovery ratio on total production is studied and the effect of low soluble salt scaling potential in feedwater on limiting the recovery is analyzed. The optimization of flow velocity and cell-pair thickness are carried out based on the total cost minimization concept before deciding the size of the system. In this way, it also covers the optimal system sizing in terms of membrane area requirement and minimum energy consumption simultaneously. The parameter values are decided based on the trade-off between fix cost and energy consumption cost of fix feed and permeate salinity. The simultaneous effect of parameter is also done in this study to get best combination of flow velocity and cell-pair thickness and finally working range of operating parameter in minimum production cost region is decided and validated with literature.

2. Design

Electrodialysis (ED) is an electro-membrane separation process in which ions are transferred through ion exchange membranes by means of a direct current (DC) voltage. ED selectively removes dissolved solids, based on their electrical charge, by transferring the brackish water ions through a semipermeable ion exchange membrane charged with an electrical potential as seen in Fig. 3. ED process technology has advanced rapidly since its inception because of improved ion exchange membrane properties, better materials of construction, advances in technology and the evolution of polarity reversal (Murray, 1995; Valero et al., 2011).

ED has many governing input variables as shown in Fig. 3 and as all these process parameters are interrelated between each other, it is necessary to choose the chronology between these design parameters and fixing some inputs to calculate all design parameters. Based on these input variables, the aim is to calculate the required membrane area, length, current, voltage and pressure drop across the ED stack.

2.1. Factors that affect ED process

To start design ED plant, feed salinity (C^{fd}) is the first parameter with us and either dilute salinity (C^{d}) or salinity difference (C^{Δ}) should be decided as per the requirement at the user end. From these data, either C^{d} or C^{Δ} is calculated by mass transfer equation (1). As ions removed from the dilute stream can go into the concentrated stream, so the salinity difference of both these streams are same by assuming both streams have equal flow rate. On the basis of any of the inlet or outlet side concentration, we can decide the other one as per the equation:

$$C^{\Delta} = C^{fd} - C^{d} = C^{c} - C^{fc} \tag{1}$$

Recovery ratio is the ratio of product water flow rate (Q^{d}) to the feedwater flow rate. As it is assumed that both streams have identical flow rate, the recovery ratio becomes 50% and for any other recovery ratio over 50%, it is necessary to operate one stream in feed-and-bleed mode. Based on the recovery ratio and equation (1), the final concentration of concentrate stream can be formulated as per the equation:

$$C^{c} = \frac{C^{fd} - RC^{d}}{1 - R} \tag{2}$$

Limiting current density is a crucial part of the design as it decides

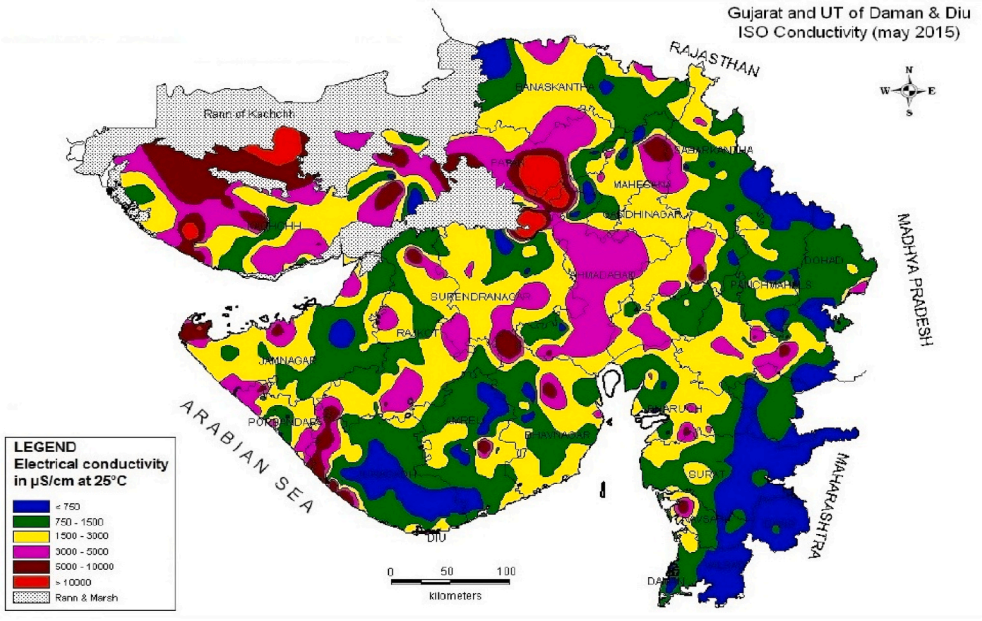

Fig. 2. Map of salinity level in Gujarat state, India (CGWB-WCR Ahmedabad, 2016).

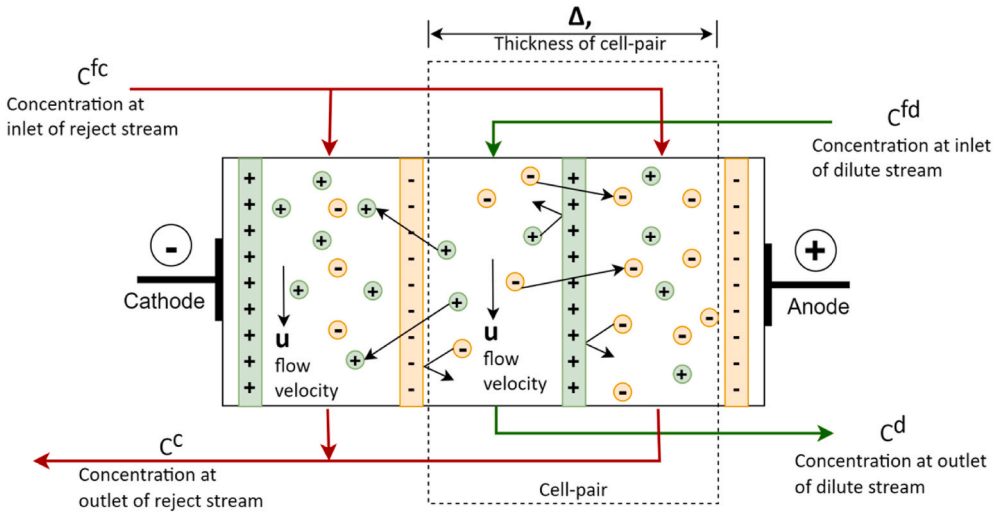

Fig. 3. Typical electrodialysis stack layout with process variables.

the maximum salt removal capacity of the system because applied current density should not be increased beyond the value of limiting current density. Limiting current density for the system is the main constraint for selecting area and length of any ED system. Limiting current density is directly proportional to the mass transfer coefficient in laminar boundary layer at the membrane surface and exit concentration of dilute stream while inversely related to the difference between the transport number of ions in the membrane and the solution. The parameter which determines the limiting current density is the mass transfer coefficient that is a function of flow velocity of solution and spacer geometry, so it is difficult to calculate the mass transfer coefficient theoretically. Practically, limiting current density is calculated based on the function developed by experimentation as a function of flow velocity of solution, type of spacer used and concentration (Lee et al., 2006).

$$i_{prac} = s\ a\ C^{d} u^{b} \tag{3}$$

After deciding all the concentration of streams, recovery ratio and limiting current density, we can calculate the membrane area and length required based on the relationship (Lee et al., 2002):

$$A_{prac} = \frac{\left[ln\left(\frac{C^{c}C^{fd}}{C^{d}C^{fc}}\right) + \frac{\Lambda\ (\rho_A+\rho_C)\left(C^{fd}-C^{d}\right)}{\Delta}\right] z\ F\ C^{d}\ Q^{d}}{\left[\frac{C^{d}}{C^{c}} + 1 + \frac{\Lambda\ C^{d}(\rho_A+\rho_C)}{\Delta}\right] i_{prac}\beta\ \varsigma} \tag{4}$$

$$L_{prac} = \frac{\left[ln\left(\frac{C^{c}C^{fd}}{C^{d}C^{fc}}\right) + \frac{\Lambda\ (\rho_A+\rho_C)\left(C^{fd}-C^{d}\right)}{\Delta}\right] z\ F\ C^{d}\ u\ \ \Delta\ \ \alpha}{\left[\frac{C^{d}}{C^{c}} + 1 + \frac{\Lambda\ C^{d}(\rho_A+\rho_C)}{\Delta}\right] i_{prac}\beta\varsigma} \tag{5}$$

where, Λ is equivalent conductance of solution, Δ is thickness of cell-pair, F is Faraday constant, α is volume factor, β area factor, s is safety factor, ς is current efficiency, $\rho_A+\rho_C$ is total membrane resistance, z is electrochemical valence.

The next step is to calculate the DC electric current and voltage. The current flow is equivalent to rate of ions transfer in solution and it is obtained by using the Faraday's law:

$$I_{st} = \frac{z\ F\ Q^{d}\ C^{\Delta}}{\varsigma N_{cp}} \tag{6}$$

The voltage is decided by the total resistance of ED cell in terms of membrane resistance as well as the resistance offered by the dilute and concentrate stream flowing in stack based on the relationship (Lee et al., 2002):

$$U_{st} = \frac{N_{cp}\ \Delta\ \ i_{prac}}{\Lambda}\left[\frac{1}{C^{c}} + \frac{1}{C^{d}} + \frac{\Lambda\ (\rho_A+\rho_C)}{\Delta}\right] \tag{7}$$

The power requirement of ED system is multiplication of current and voltage while specific power energy per unit volume of water produced is calculated by the equation:

$$E_{des} = \frac{P_{des}\alpha}{1000\ Q^{d}\ \times 3600} \tag{8}$$

The pumping energy required is calculated by the pressure drop in ED stack and efficiency of pump (η_p). Pressure drop is calculated based on relation (Tsiakis and Papageorgiou, 2005):

$$\Delta P = \frac{32 u L_{prac}\mu}{\left(d^{H}\right)^{2}} \tag{9}$$

$$d^{H} = \frac{8 - 4\pi\frac{h}{l}}{\frac{4}{w} + \frac{1}{h} + 2\pi\left(1 - \frac{h}{w}\right)\frac{1}{l}} \tag{10}$$

where μ is the viscosity of the solution used in the system, d^H is the hydraulic diameter, h is half thickness of grid rod in spacer, l is mesh size, w is the width of cell-pair.

The pumping energy required per unit volume of water produced is given by equation:

$$E_{pump} = \frac{\Delta P}{3600\ \eta_p} \tag{11}$$

2.2. Design methodology and sample calculation

The membrane area and length obtained earlier is the total size required for ED stack consisting only single cell-pair. But the length and width of the ED stack is very large compared to the system overall size which is to be reduced to make it practically possible to assemble stack. As per the size available at manufacturer's end, the length and width of stack obtained will be divided into the number of hydraulic stage and number of cell-pair respectively. If this number of stage and cell-pair is not obtained as integer value then recalculation would be done as per the step of back calculation shown in Fig. 4.

Based on the proposed mathematical formulation, the sample calculation is done for the design of pilot scale ED plant of 500 L/h capacity with 70% recovery to produce potable water. The feedwater composition which is characterized by CSIR-NEERI (Council of Scientific and Industrial Research- National Environmental Engineering Research

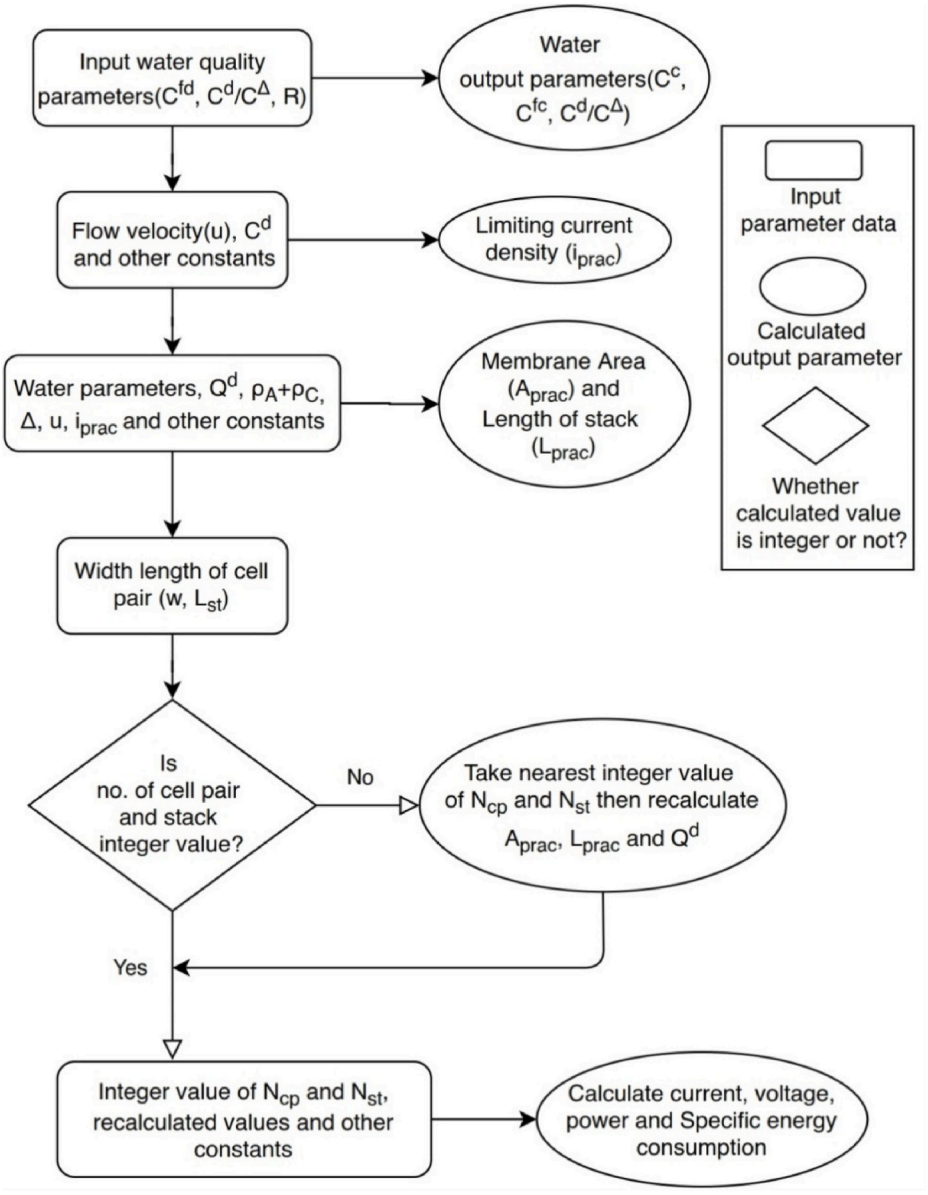

Fig. 4. Flow chart for the calculation steps to design electrodialysis system.

Institute), Nagpur, India, is shown in Table 1 with the calculated input and output parameters of ED system design. The values obtained for the number of cell-pair and stages are non-integer so back calculation is done and values for the parameter obtained is shown in Table 2.

The schematic flow diagram is shown in Fig. 5 as per the design and calculated value of the proposed electrodialysis plant.

Assumptions of design are:

- Dilute and concentrate cells have identical geometries,
- The flow streams of dilute and concentrate are co-current and of equal velocity,
- The activity coefficients of the salt in the dilute and concentrate are 1,
- Concentration potentials and boundary layer effects are neglected,
- The osmotic and electro-osmotic effect of water transport is neglected.

Membrane properties, limited current density constants, current efficiency are taken from the literature (Strathmann, 2004).

3. Optimization of electrodialysis process parameters

3.1. Assumption of cost analysis

The total cost of ED is the sum of fixed cost associated with amortization of the plant capital cost and plant's operating cost. The fixed cost has cost of ED stack which is around 45–50% of total cost of system (Nayar et al., 2017). This stack cost is directly related to membrane area and stack cost, including membrane, is 1.5 times membrane cost (Lu et al., 2016). The peripheral equipment cost accounts for 0.5 times the stack cost. Total capital cost is the sum of stack cost and peripheral equipment cost. While operating cost includes two energy consumptions one is DC current given to ED stack and another is pump energy consumption. This energy consumption is governed by equations (8) and (11). The economic data for the ED is given in Table 3.

To operate ED plant with better efficiency and with minimum possible fix investment, it is required to optimize the ED process with governing parameters of recovery ratio, flow velocity and cell-pair thickness.

Table 1
Sample calculation for PDEU groundwater quality for pilot scale ED plant.

PDEU groundwater characterization			Input Data			Output Data		
Parameter	Value	Unit	Symbol	Value	Unit	Symbol	Value	Unit
pH	8.9		C^{fd}	1100	mg/L	C^{Δ}	1000	mg/L
TDS	1100	mg/L	C^{d}	100	mg/L	C^{c}	4100	mg/L
Calcium	11	mg/L	R	0.70		C^{fc}	3100	mg/L
Total hardness as $CaCO_3$	104	mg/L	Λ	10.5	Sm^2/keq for NaCl	i_{emp}	11.41	A/m^2
Magnesium	18	mg/L	Δ	0.0005	m	i_{prac}	7.98	A/m^2
Sodium	348	mg/L	u	0.15	m/s	A_{prac}	12.19	m^2
Potassium	3	mg/L	a	25000	$As^bm^{(1-b)}$/keq	2A	24.38	m^2
Total alkalinity as $CaCO_3$	450	mg/L	b	0.5		L_{prac}	3.42	m
			F	96500000	As/keq	N_{cp}	35.61	nos.
			α	0.8		N_{st}	8.15	nos.
			β	0.7		I_{st}	6.97	A
			s	0.7		U_{st}	11.02	V
			ς	0.9		P_{des}	76.82	W
			$\rho_A+\rho_C$	0.0007	Ω m^2	E_{des}	0.14	kWh/m^3
			Q^{d}	500	L/h	E_{pump}	0.14	kWh/m^3
			w	0.1	m	E_{total}	0.28	kWh/m^3
			L_{st}	0.42	m			
			ΔP	150	kPa			
			η_p	0.6				

Table 2
Re-calculated value after taking integer value for number of cell-pair and stage.

Integer value taken			Re-calculated output values					
Symbol	Value	Unit	Symbol	Value	Unit	Symbol	Value	Unit
N_{cp}	36	nos.	A_{prac}	12.10	m^2	I_{st}	6.89	A
N_{st}	8	nos.	2A	24.20	m^2	U_{st}	11.14	V
			L_{prac}	3.36	m	P_{des}	76.82	W
						E_{des}	0.12	kWh/m^3

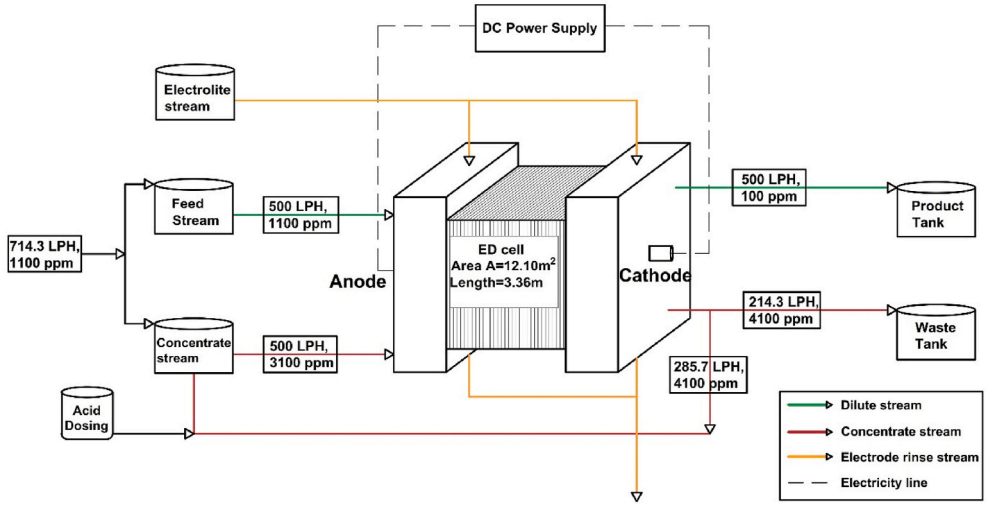

Fig. 5. Schematic flow diagram of proposed electrodialysis design.

Table 3
Calculation assumption for the cost analysis for ED system.

Items	Cost	Unit
Membrane cost	25	USD/m^2
Membrane life	5	Years
Stack cost	1.5	times membrane cost
Peripheral equipment cost	0.5	times stack cost
Electricity cost	0.1	USD/kWh

3.2. Recovery ratio optimization

As the concentrate stream is operated in feed-and-bleed mode, the recovery ratio is increased by increasing the recirculation of concentrate stream. Through ED system, recovery ratio can be achieved as high as 95% but there are some limitations for the recovery ratio due to sparingly soluble salt present in feedwater.

As the salinity of concentration stream is a function of recovery ratio as per equation (2), increase in water recovery will result in increasing the salinity of concentrate stream. The higher the salinity in concentrate stream, the lower the electrical resistance due to the available ions to

carry current is high. This faster movement of ions in transport of salinity from dilute to concentrate stream leads to the reduced length requirement as per equation (5) which reduces the membrane area requirement as presented in Fig. 6 (A) with black color.

As the width of stack is unaffected, the volume flow rate of system remains same, while the reduction in flow length offers less flow resistance and so the pressure drop in stack reduces. Here pumping power requirement reduces as per equations (9) and (11). The lower electrical resistance at higher concentration also reduces energy consumption in stack due to less potential difference required to draw same current which is as per equation (7) and this observation is in line with previously published work (Dai et al., 2019; Silva et al., 2013). This trend of energy consumption is shown in Fig. 6 (A) with red color. The total cost, which is sum of capital cost and energy cost, reduces with the increase in recovery ratio and shown in Fig. 6 (B).

As fix cost and variable cost have the same trend in relation with recovery ratio, the limiting criteria for the recovery ratio cannot be decided based on the total cost parameter. Only limiting criteria is low water-soluble calcium salt (calcium carbonate and calcium sulfate) precipitation at high recovery ratio because of high concentration. Scaling potential of calcium carbonate is indicated by the LSI (Langelier Saturation Index) value.

LSI value is difference between two pH values one is actual pH of water and other is pH value at which calcium carbonate scaling starts (Raich-Montiu et al., 2014). At pH 6.5 to 9.5, the LSI is used to show the scaling potential of water containing carbonates which is expressed by

$$LSI = pH - pH_s \quad (12)$$

where pH is the measured feedwater pH and pH_s is the "saturation pH" at which the water is saturated with calcium carbonate. pH_s is defined as

$$pH_s = (9.3 + A + B) - (C + D) \quad (13)$$

Where $A = (\log_{10}[TDS] - 1)/10$, [TDS] is the concentration of total dissolved solids (mg/L); $B = -13.12 \times \log_{10}(T) + 34.55$, T is the Kelvin temperature (K); $C = \log_{10}[C^*_{Ca^{2+}}] - 0.4$, $[C^*_{Ca^{2+}}]$ is the concentration of Ca^{2+} as $CaCO_3$ (mg/L); $D = \log_{10}[Alk]$, [Alk] is the concentration of alkalinity as $CaCO_3$ (mg/L) (Raich-Montiu et al., 2014).

Improved LSI by Carrier gives detailed indication for range of LSI values as shown in Table 4. LSI value of concentrated water should be less than zero (target LSI value should be minus 0.2 as per Lenntech-Hydranautics membrane information) (Bates, 2001) to eliminate risk of calcite scaling in ED stack.

As the LSI value calculated is 0.9 for brackish water source data of Table 1 and it is more than zero, the scaling potential for this feedwater is high. The scaling of calcium carbonate depends upon the pH and temperature of water. Secondly, carbonate ion continuously migrates from the dilute to concentrate compartment so dilute compartment will not require any pH adjustment. To reduce scaling potential of concentrate compartment, it is recommended to acidify the concentrate stream and reduce the pH which can decrease the scaling potential of water (Zhang et al., 2011).

Table 4
Improved LSI indication for range of values (Lenntech, 2019).

LSI (Carrier)	Indication
−2.0< LSI < -0.5	Serious corrosion
−0.5 < LSI<0.0	Slightly corrosion but non-scale forming
LSI = 0.0	Balanced but pitting corrosion possible
0.0 < LSI<0.5	Slightly scale forming and corrosive
0.5 < LSI<2.0	Scale forming but non corrosive

pH of water can be reduced up to the neutral pH (7 pH) which is the natural pH value of water below which water becomes acidic (Prihasto et al., 2009). So at neutral pH and for different concentration of reject water according to different recovery ratio, the LSI value is calculated and mentioned in Table 5. Increasing recovery ratio increases the LSI value from −0.52 to −0.19 at 70% recovery ratio. Based on this LSI value, the maximum attainable recovery is 70–75% after acid dosing as a pretreatment for the 1100 ppm feedwater.

3.3. Flow velocity optimization

The flow velocity of solution in ED cell is an important parameter to decide the limiting current density, area of membrane and current requirement, so it is needed to optimize the flow velocity with respect to membrane cost and energy requirement for desalination.

Increasing flow velocity allows the higher limiting current density because limiting current is directly proportional to velocity as per equation (3) which will lead to the decreasing the required membrane area as per equation (4) for the constant production capacity. This reduction of membrane area and so the capital cost is shown in Fig. 7 (A).

Table 5
LSI value at 7 pH for different recovery ratio.

Recovery Ratio	Concentrate stream outlet salinity, C^c (ppm)	LSI at 7 pH
50%	2100	−0.52
55%	2322	−0.45
60%	2600	−0.37
65%	2957	−0.29
70%	3433	−0.19
75%	4100	−0.07

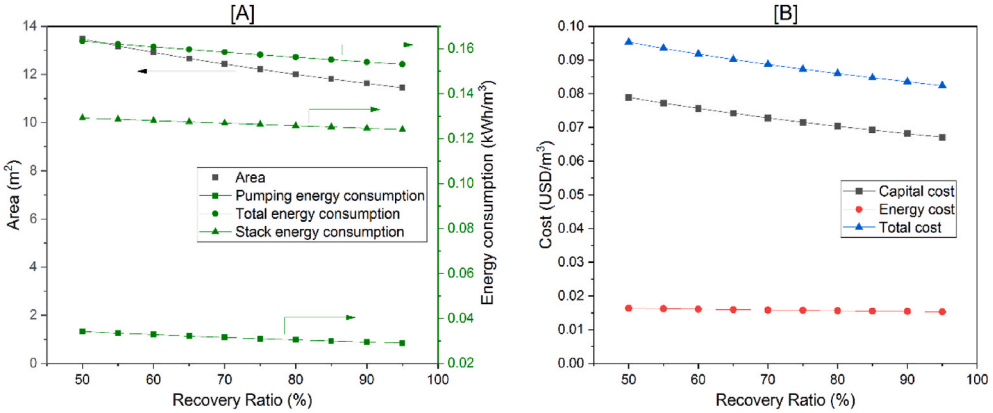

Fig. 6. The effect of recovery ratio on A) Area and various energy consumption, B) capital, energy and total cost.

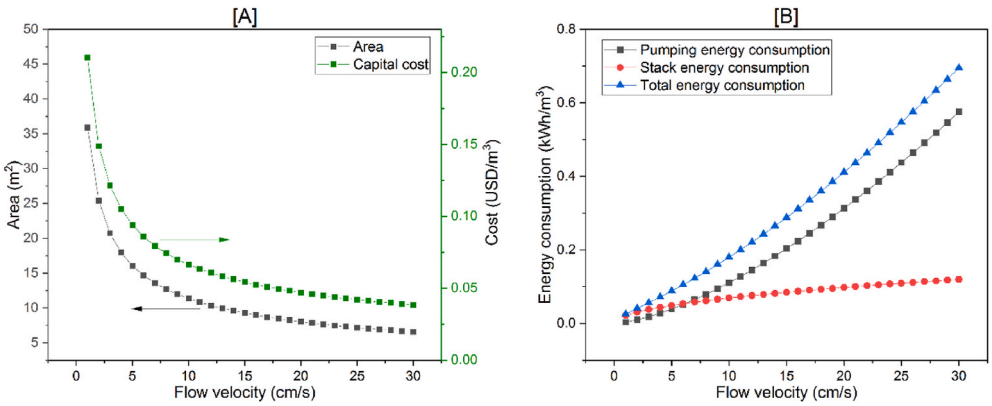

Fig. 7. Effect of flow velocity on A) membrane area and capital cost, B) pumping, stack and total energy consumption.

Increase in flow velocity requires increasing in the current in ED cell for same amount of ion removal. This phenomenon can also be understood as a reduced 'total area' reflects in small number of cell-pair in stack which leads to increasing in current requirement as per equation (6). This increase in current leads to an increased power requirement for desalination. High flow velocity also increases the pump energy requirement because it increases the pressure drop in ED cell as seen in equation (9). So total energy requirement, which is a sum of stack and pumping energy, increases with flow velocity and presented in Fig. 7 (B). This phenomenon of energy consumption is similar with the previously reported for high-salinity brine (Chehayeb et al., 2017).

As shown in Fig. 8, the total production cost, which is the sum of capital and energy cost, first decreases rapidly up to the 13 cm/s flow velocity because in this region the capital cost is dominantly high compare to the energy cost. Also, the capital cost decreases rapidly compared to an almost linear increment of energy cost. After 13 cm/s flow velocity, decrement in capital cost is very low while in the same region the energy cost steadily increases and also crosses the value of capital cost after 20 cm/s flow velocity. The overall result is that the total cost starts increasing after flow velocity of 13 cm/s and at this flow velocity, the total cost become minimum and 13 cm/s flow velocity is an optimum value for the feedwater of 1100 mg/L concentration.

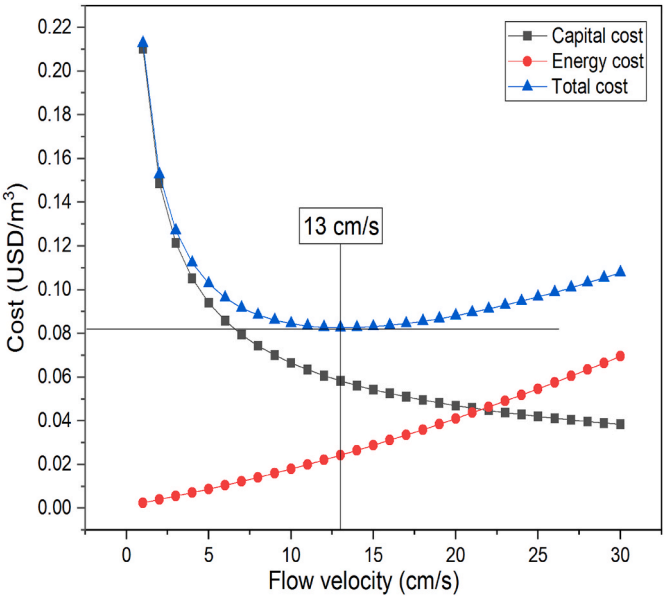

Fig. 8. Capital cost, energy cost and total cost varies with flow velocity.

3.4. Cell thickness optimization

As the cell-pair thickness increases, the membrane area requirement decreases as per equation (4). At higher cell-pair thickness, the flow channel cross-sectional area increases and allows higher volume flow rate at same flow velocity so it requires less membrane width and ultimately reduce the total membrane area requirement for same flow capacity. This decrease in membrane area also results in to lower capital cost with higher cell-pair thickness which is shown in Fig. 9 (A).

As cell-pair thickness increases, the electrical resistance offered by the solution flowing in the channel between two membranes also increases due to the longer path for the current flow. So for the same flow speed, voltage requirement needs to be increased to overcome the increased resistance of the system. This increase in voltage results in to increase of energy consumption in ED stack. The pumping energy requirement directly related to the pressure drop in the stack which depends on two parameters one is flow length of stack and another is equivalent hydraulic diameter of flow channel. Increase in cell-pair thickness increases the hydraulic diameter as well as increases the flow length of the ED stack as per equation (5) and both parameter increases linearly. Pressure drop increases with increase in flow length but decreases as power function as per equation (9). As shown in Fig. 9 (B), the total energy consumption, which is the sum of pumping and stack energy consumption, decreases rapidly with increment of cell-pair thickness up to the 0.4 mm where pumping energy requirement is high compare to the stack energy consumption. After 0.4 mm thickness, the total energy consumption starts increasing with cell-pair thickness because of a steady increment of stack energy compare to low pumping energy consumption.

As shown in Fig. 10, with increment of cell-pair thickness up to 0.4 mm, the energy cost decreases rapidly and so the total cost which is also supported by the reduction in capital cost. After 0.4 mm cell-pair thickness, energy cost increases while capital cost is still decreases but at a slower rate which leads to the total cost become minimum at 0.51 mm cell-pair thickness and increases thereafter.

3.5. Simultaneous effect of flow velocity and cell-pair thickness on total production cost

From this velocity and cell thickness optimization, it is seen that both the values are simultaneously affecting the total cost of ED unit. To find best operating flow velocity and cell-pair size, it is necessary to study the effect of both parameters at a time. To fulfill this aim, multiple graph of fluid velocity vs. total cost are plotted at a different value of cell-pair thickness and shown in Fig. 11. This simulation is obtained by using nested for loop in MATLAB software by nesting the cell-pair thickness over the flow velocity loop.

It is observed from previous Figs. 7 and 9 that the capital cost is

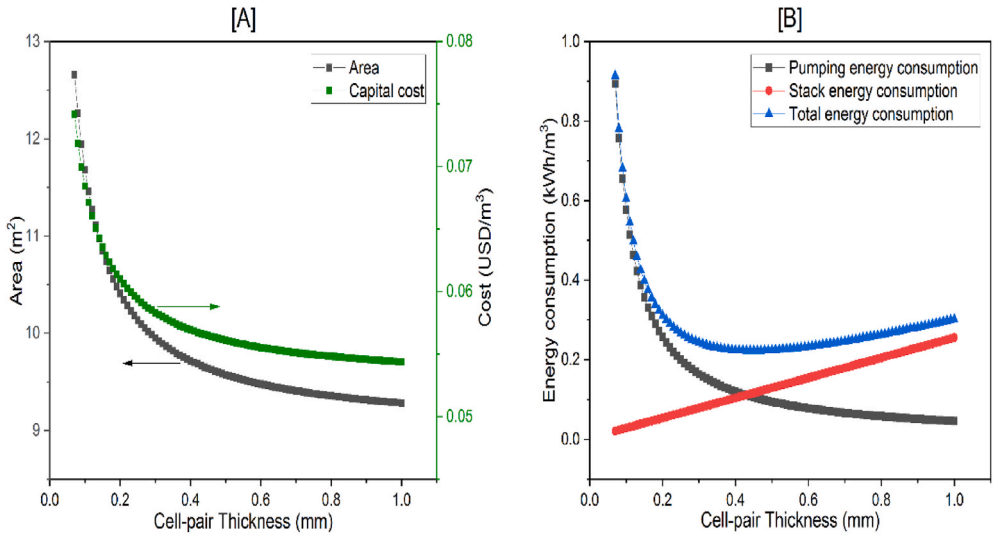

Fig. 9. Effect of cell-pair thickness on A) membrane area and capital cost, B) pumping, stack and total energy consumption.

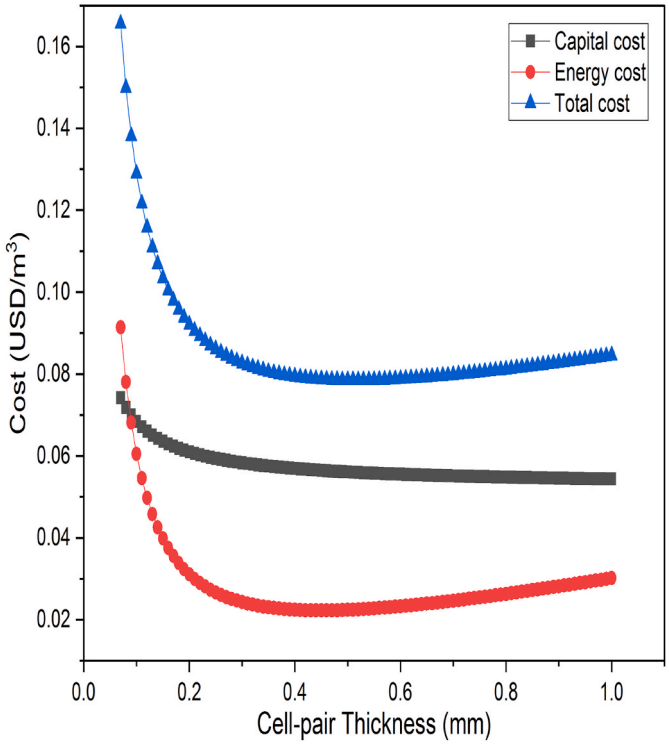

Fig. 10. Effect of cell-pair thickness on the cost of water production.

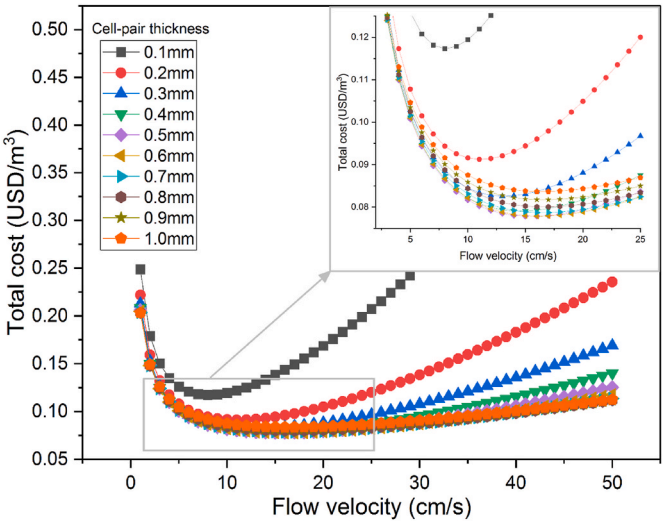

Fig. 11. Simultaneous effect of flow velocity and cell-pair thickness on total production cost.

always decreases either by increasing flow velocity or cell-pair thickness. This reduction is rapid at lower values of flow velocity and cell-pair thickness and afterwards trend continues but at a slower rate. So in obtaining minimum total cost, the role of energy cost is vital. At flow velocity less than 10 cm/s, the energy cost is higher than capital cost for cell-pair thickness less than 0.1 mm due to huge pressure drop in flow channel but this energy cost reduces fast by increasing cell-pair thickness up to 0.4 mm as seen in Fig. 10. After increasing flow velocity over 20 cm/s, the energy cost reaches higher than capital cost as per the discussion of Fig. 8, this trend is sharper at lower cell-pair thickness below 0.2 mm so the minimum total production cost is obtained at lower flow velocity less than 10 cm/s as seen in Fig. 11.

For the cell-pair thickness more than 0.2 mm, the optimum flow velocity value shifts towards right side and found between 10 and 20 cm/s. This is because of reduction in energy cost, due to increasing cell-pair thickness more than 0.2 mm, would not compensate by increasing flow velocity from 10 to 20 cm/s. At the same time, total cost at optimum point is also reducing because total cost is minimum between 10 and 20 cm/s flow velocity as seen in Fig. 8.

From the above discussion of cell-pair thickness and flow velocity simultaneous optimization, it is observed that for various cell thickness values, the optimum value of flow velocity ranges from 8 to 17 cm/s as mentioned in Table 6. It is also observed that minimum cost per unit output is lowest at the cell thickness of 0.5 mm and flow velocity of 16 cm/s and least cost is 7.786 USD per 100 m^3 of pure water produced. This cost is lower than water cost of 0.12 USD/m^3 produced by conventional RO treatment for the feed of 1500 ppm and product of 500 ppm, reported in recent study (Liu et al., 2021). It is recommended to choose the cell thickness between 0.4 and 0.8 mm as per the availability and ED unit size because production cost increase from lowest value is within 3% only. This range of cell-pair thickness concluded here is within the range of 0.2–1.0 mm reported by other (Hattenbach and Kneifel, 1986) however the optimum value obtained by them is 0.2 mm

Table 6
Optimum flow velocity value for different cell thickness.

Cell-pair thickness (mm)	0.1	0.2	0.3	0.4	0.5	0.6	0.7	0.8	0.9	1.0
Optimum Flow velocity (cm/s)	8	11	13	15	16	16	16	17	17	16
Total Cost (USD per 100 m^3)	11.73	9.13	8.26	7.91	7.78	7.79	7.87	8.01	8.17	8.37

which is lower than the observed here. The optimum cell-pair thickness value of 0.5 mm is also obtained in previous recent study by considering only the operating cost and high salt removal (Chehayeb et al., 2017). In this range of cell-pair thickness, the optimum flow velocity falls within a range of 15–17 cm/s which is more narrow range than 13–17 cm/s reported by the previous study (Hattenbach and Kneifel, 1986). But in previous study, the cost is decreasing continuously with the cell-pair thickness would be because of considering higher membrane cost while in this study, the optimum cell-pair thickness shift right side at 0.5 mm by considering pumping power in total energy cost.

4. Conclusion

The design calculations of the ED system suggest that the pumping power is equally important with stack energy consumption for the low salinity feed ED application. The Specific Energy Consumption (SEC) calculated for PDEU groundwater is 0.28 kWh/m^3 in which 50% of energy is consumed by pumps.

The recovery ratio can be adjusted to 70%–75% for the safe running of ED unit in terms of scaling. It is achieved by reducing feedwater pH to 7 using acid dosing. For reducing the waste stream generation, the recovery ratio needs to be increased, but it is limited by the scaling potential of feedwater.

The capital cost increases sharply below 7 cm/s flow velocity and downfall is very low after 15 cm/s. The energy cost continuously increases with the flow velocity due to increase in pressure drop. This trade-off between capital cost and energy cost results in minimum total cost at 13 cm/s flow velocity.

In the case of cell-pair thickness, up to 0.3 mm, the capital cost and pumping energy cost decreases sharply and continue to decrease further beyond 0.3 mm but at a slower rate. The stack energy cost increases linearly in entire range of 0.07–1.0 mm cell-pair thickness. So the total cost reduces sharply up to 0.3 mm and starts increasing after 0.6 mm, which results in minimum total cost at 0.51 mm cell-pair thickness.

The simultaneous parametric study concluded that the optimized working range for cell-pair thickness is 0.4–0.8 mm and flow velocity is 15–17 cm/s in which the production cost increases only within 3% from the minimum cost of 7.786 USD per 100 m^3 of water produced. This minimum cost is obtained at the cell-pair thickness of 0.5 mm and flow velocity of 16 cm/s.

Further, this study can be extended by applying optimization in innovative and non-conventional ED stack configuration to reduce the total cost. The more rigorous mathematical model, having osmotic and electro-osmotic water transport through the membrane, can make further critical analysis.

Declaration of competing interest

The authors declare that they have no known competing financial interests or personal relationships that could have appeared to influence the work reported in this paper.

Acknowledgement

Authors acknowledge the project grant received from the European Union's Horizon 2020 research and innovation programme under grant agreement No 820906 and the Department of Biotechnology, Government of India, Project no: BT/IN/EU-WR/40/AM/2018. Infrastructural facilities provided by Pandit Deendayal Energy University, Gujarat, India are also deeply acknowledged.

References

CGWB-WCR Ahmedabad, 2016. Groundwater Year Book, 2015-16, Gujarat State and UT of Daman & Diu, CGWB. Ministry of Water Resources, RD & GR, Government of India.

Al-Amshawee, S., Yunus, M.Y.B.M., Azoddein, A.A.M., Hassell, D.G., Dakhil, I.H., Hasan, H.A., 2020. Electrodialysis desalination for water and wastewater: a review. Chem. Eng. J. 380 https://doi.org/10.1016/j.cej.2019.122231.

Ali, A., Tufa, R.A., Macedonio, F., Curcio, E., Drioli, E., 2018. Membrane technology in renewable-energy-driven desalination. Renew. Sustain. Energy Rev. 81 https://doi.org/10.1016/j.rser.2017.07.047.

AlMarzooqi, F.A., Al Ghaferi, A.A., Saadat, I., Hilal, N., 2014. Application of Capacitive Deionisation in water desalination: a review. Desalination 342. https://doi.org/10.1016/j.desal.2014.02.031.

Bates, W., 2001. RO water chemistry. Hydranautics - A Nitto Group Company technical paper [WWW Document]. URL. https://membranes.com/docs/papers/04_ro_water_chemistry.pdf. (Accessed 2 February 2021). accessed.

Campione, A., Gurreri, L., Ciofalo, M., Micale, G., Tamburini, A., Cipollina, A., 2018. Electrodialysis for water desalination: a critical assessment of recent developments on process fundamentals, models and applications. Desalination 434. https://doi.org/10.1016/j.desal.2017.12.044.

Chehayeb, K.M., Farhat, D.M., Nayar, K.G., Lienhard, J.H., 2017. Optimal design and operation of electrodialysis for brackish-water desalination and for high-salinity brine concentration. Desalination 420. https://doi.org/10.1016/j.desal.2017.07.003.

Chen, Q.B., Wang, J., Liu, Y., Zhao, J., Li, P., 2020. Novel energy-efficient electrodialysis system for continuous brackish water desalination: innovative stack configurations and optimal inflow modes. Water Res. 179 https://doi.org/10.1016/j.watres.2020.115847.

Dai, K., Wen, J.L., Wang, Y.L., Wu, Z.G., Zhao, P.J., Zhang, H.H., Wang, J.J., Zeng, R.J., Zhang, F., 2019. Impacts of medium composition and applied current on recovery of volatile fatty acids during coupling of electrodialysis with an anaerobic digester. J. Clean. Prod. 207 https://doi.org/10.1016/j.jclepro.2018.10.019.

Faridabad, C.G.W.B., 2018. Ground Water Quality in Shallow Aquifers in India, CGWB. Ministry of Water Resources RD & GR, Government of India.

Ghyselbrecht, K., Huygebaert, M., Van der Bruggen, B., Ballet, R., Meesschaert, B., Pinoy, L., 2013. Desalination of an industrial saline water with conventional and bipolar membrane electrodialysis. Desalination 318. https://doi.org/10.1016/j.desal.2013.03.020.

Hanrahan, C., Karimi, L., Ghassemi, A., Sharbat, A., 2016. High-recovery electrodialysis reversal for the desalination of inland brackish waters. Desalin. Water Treat. 57 https://doi.org/10.1080/19443994.2015.1041162.

Hattenbach, K., Kneifel, K., 1986. The effect of cell thickness and flow velocity on water cost in desalination by electrodialysis. Desalination 58. https://doi.org/10.1016/0011-9164(86)85010-X.

He, W., Buonassisi, T., Peters, I.M., Winter, A.G.V., 2018a. System-Level Cost and Performance Optimization for Photovoltaic-Powered Electrodialysis Reversal Desalination, Desalination and Water Purification Research and Development Program Report No. 210.

He, W., Buonassisi, T., Wright, N.C., Peters, I.M., Amrose, S., Winter, A.G.V., 2018b. Preliminary field test results from a photovoltaic electrodialysis brackish water desalination system in rural India. Proceedings of the ASME Design Engineering Technical Conference. https://doi.org/10.1115/DETC201886183.

Karimi, L., Ghassemi, A., 2016. Effects of operating conditions on ion removal from brackish water using a pilot-scale electrodialysis reversal system. Desalin. Water Treat. 57 https://doi.org/10.1080/19443994.2015.1024748.

Karimi, L., Abkar, L., Aghajani, M., Ghassemi, A., 2015. Technical feasibility comparison of off-grid PV-EDR and PV-RO desalination systems via their energy consumption. Separ. Purif. Technol. 151 https://doi.org/10.1016/j.seppur.2015.07.023.

Karimi, L., Ghassemi, A., Zamani Sabzi, H., 2018. Quantitative studies of electrodialysis performance. Desalination 445. https://doi.org/10.1016/j.desal.2018.07.034.

Landsman, M.R., Lawler, D.F., Katz, L.E., 2020. Application of electrodialysis pretreatment to enhance boron removal and reduce fouling during desalination by nanofiltration/reverse osmosis. Desalination 491. https://doi.org/10.1016/j.desal.2020.114563.

Lee, H.J., Sarfert, F., Strathmann, H., Moon, S.H., 2002. Designing of an electrodialysis desalination plant. Desalination 142. https://doi.org/10.1016/S0011-9164(02)00208-4.

Lee, H.J., Strathmann, H., Moon, S.H., 2006. Determination of the limiting current density in electrodialysis desalination as an empirical function of linear velocity. Desalination 190. https://doi.org/10.1016/j.desal.2005.08.004.

Lenntech, B.V., 2019. Langelier Saturation Index Calculator [WWW Document]. URL. https://www.lenntech.com/calculators/langelier/index/langelier.htm. (Accessed 2 February 2021). accessed.

Liu, X., Shanbhag, S., Bartholomew, T.V., Whitacre, J.F., Mauter, M.S., 2021. Cost comparison of capacitive deionization and reverse osmosis for brackish water desalination. ACS ES&T Eng. 1 https://doi.org/10.1021/acsestengg.0c00094.
Lu, H., Zou, W., Chai, P., Wang, J., Bazinet, L., 2016. Feasibility of antibiotic and sulfate ions separation from wastewater using electrodialysis with ultrafiltration membrane. J. Clean. Prod. 112 https://doi.org/10.1016/j.jclepro.2015.09.091.
Malmrose, P., Lozier, J., Mickley, M., Reiss, R., Russell, J., Schaefer, J., Sethi, S., Manuszak, J., 2004. Committee report: current perspectives on residuals management for desalting membranes. Am. Water Works Assoc. J. 96, 73–87. https://doi.org/10.1002/j.1551-8833.2004.tb10760.x.
Murray, P. (Ed.), 1995. Electrodialysis and Electrodialysis Reversal: M38, First. American Water Works Association.
Myint, M.T., Ghassemi, A., Nirmalakhandan, N., 2010. Design of ILEDR for brackish groundwater: a literature review approach. Desalin. Water Treat. 24 https://doi.org/10.5004/dwt.2010.1482.
Nayar, K.G., Sundararaman, P., O'Connor, C.L., Schacherl, J.D., Heath, M.L., Gabriel, M. O., Shah, S.R., Wright, N.C., Winter Amos, G.V., 2017. Feasibility study of an electrodialysis system for in-home water desalination in urban India. Dev. Eng. 2, 38–46. https://doi.org/10.1016/j.deveng.2016.12.001.
Nicot, J.P., Chowdhury, A.H., 2005. Disposal of brackish water concentrate into depleted oil and gas fields: a Texas study. Desalination 181. https://doi.org/10.1016/j.desal.2005.02.013.
Patel, S.K., Qin, M., Walker, W.S., Elimelech, M., 2020. Energy efficiency of electro-driven brackish water desalination: electrodialysis significantly outperforms membrane capacitive deionization. Environ. Sci. Technol. 54 https://doi.org/10.1021/acs.est.9b07482.
Prihasto, N., Liu, Q.F., Kim, S.H., 2009. Pre-treatment strategies for seawater desalination by reverse osmosis system. Desalination 249. https://doi.org/10.1016/j.desal.2008.09.010.
Qu, J.X., Liu, S.M., 1983. Electrode for electrodialysis. Desalination 46. https://doi.org/10.1016/0011-9164(83)87160-4.
Qureshi, B.A., Qasem, N.A.A., Zubair, S.M., 2021. Normalized sensitivity analysis of electrodialysis desalination plants for mitigating hypersalinity. Separ. Purif. Technol. 257 https://doi.org/10.1016/j.seppur.2020.117858.
Raich-Montiu, J., Barios, J., Garcia, V., Medina, M.E., Valero, F., Devesa, R., Cortina, J.L., 2014. Integrating membrane technologies and blending options in water production and distribution systems to improve organoleptic properties. The case of the Barcelona Metropolitan Area. J. Clean. Prod. 69 https://doi.org/10.1016/j.jclepro.2014.01.032.
Shah, S.R., Wright, N.C., Nepsky, P.A., Winter, A.G., 2018. Cost-optimal design of a batch electrodialysis system for domestic desalination of brackish groundwater. Desalination 443. https://doi.org/10.1016/j.desal.2018.05.010.
Silva, V., Poiesz, E., van der Heijden, P., 2013. Industrial wastewater desalination using electrodialysis: evaluation and plant design. J. Appl. Electrochem. 43, 1057–1067. https://doi.org/10.1007/s10800-013-0551-4.
Strathmann, H., 2004. Ion-exchange membrane process and equipment design. Membrane Science and Technology, pp. 227–286. https://doi.org/10.1016/S0927-5193(04)80036-6.
Strathmann, H., 2010. Electrodialysis, a mature technology with a multitude of new applications. Desalination 264. https://doi.org/10.1016/j.desal.2010.04.069.
Tsiakis, P., Papageorgiou, L.G., 2005. Optimal design of an electrodialysis brackish water desalination plant. Desalination 173. https://doi.org/10.1016/j.desal.2004.08.031.
Turek, M., Dydo, P., 2003. Electrodialysis reversal of calcium sulphate and calcium carbonate supersaturated solution. Desalination 158. https://doi.org/10.1016/S0011-9164(03)00438-7.
Valero, F., Barcelo, A., Arbos, R., 2011. Electrodialysis technology - theory and applications. In: Michael, S. (Ed.), Desalination, Trends and Technologies. InTech. https://doi.org/10.5772/14297.
Walha, K., Amar, R. Ben, Firdaous, L., Quéméneur, F., Jaouen, P., 2007. Brackish groundwater treatment by nanofiltration, reverse osmosis and electrodialysis in Tunisia: performance and cost comparison. Desalination 207. https://doi.org/10.1016/j.desal.2006.03.583.
Walker, W.S., Kim, Y., Lawler, D.F., 2014. Treatment of model inland brackish groundwater reverse osmosis concentrate with electrodialysis-Part I: sensitivity to superficial velocity. Desalination 344. https://doi.org/10.1016/j.desal.2014.03.035.
Watson, I.C., Morin, O.J., Henthorne, L., 2003. Desalting Handbook for Planners, Desalination and Water Purification Research and Development Program Report No. 72.
Wright, N.C., Van De Zande, G., Winter, A.G., 2015. Justification, design, and analysis of a village-scale photovoltaic-powered electrodialysis reversal system for rural India. Proceedings of the ASME Design Engineering Technical Conference. https://doi.org/10.1115/DETC201546521.
Zhang, Y., Ghyselbrecht, K., Meesschaert, B., Pinoy, L., Van der Bruggen, B., 2011. Electrodialysis on RO concentrate to improve water recovery in wastewater reclamation. J. Membr. Sci. 378 https://doi.org/10.1016/j.memsci.2010.10.036.

Symbols

C^{fd}: Concentration at inlet of dilute stream, keq/m^3
^{Cd}: Concentration at exit of dilute stream, keq/m^3
R: Recovery
Λ: Equivalent conductance of solution at 20 °C, Sm^2/keq
Δ: Thickness of cell-pair, m
u: Linear flow velocity, m/s
a: Constant for limiting current density calculation, As^{b}m$^{(1-b)}$/keq
b: Constant for limiting current density calculation
F: Faraday constant, As/keq
α: Volume factor
β: Area factor accounting for shadow effect
s: Safety factor
ς: Current utilization/efficiency
$\rho_A+\rho_C$: Total area resistance of membrane, Ω m^2
Q^d: Product water flow rate (Production capacity), m^3/s
w: Width of cell-pair, m
L_{st}: Length of flow path per stack, m
h: Half thickness of the grid rods of spacer, m, (h = 1/4 Δ)
l: Distance between two grid rods or mesh size, m
μ: Solution viscosity, kg/m-s
d^H: Hydraulic diameter, m
η_p: Efficiency of pump
C^{Δ}: Concentration difference of dilute/concentration stream, keq/m^3
C^{fc}: Concentration at inlet of concentrate stream, keq/m^3
C^c: Concentration at exit of concentrate stream, keq/m^3
ΔP: Pressure drop in stack, kPa
i_{emp}: Empirical limiting current density, A/m^2
i_{prac}: Practical limiting current density, A/m^2
A_{prac}: Area required for stack, m^2
L_{prac}: Total Length required, m
N_{cp}: No of cell-pairs in stage
N_{st}: No of stage
I_{st}: Current passing through stack, A
U_{st}: Potential(Voltage) drop across stack, V
P_{des}: Power required for desalination, W
E_{des}: Specific energy consumption for desalination, kWh/m^3
E_{pump}: Specific energy consumption for pump, kWh/m^3
E_{total}: Total Specific energy consumption for ED unit, kWh/m^3